soils

MDPI

Article

Ectomycorrhizal Fungi and Mineral Interactions in the Rhizosphere of Scots and Red Pine Seedlings

Zsuzsanna Balogh-Brunstad [1,*], C. Kent Keller [2], Zhenqing Shi [3], Håkan Wallander [4] and Susan L. S. Stipp [5]

1 Departments of Chemistry, Geology and Environmental Sciences, Hartwick College, Oneonta, NY 13820, USA
2 School of the Environment, Washington State University, Pullman, WA 99164, USA; ckkeller@wsu.edu
3 School of Environment and Energy, South China University of Technology, Guangzhou 510006, China; zqshi@scut.edu.cn
4 Microbial Ecology, Department of Biology, Lund University, 22362 Lund, Sweden; hakan.wallander@biol.lu.se
5 Nano-Science Center, Department of Chemistry, University of Copenhagen, 2100 Copenhagen, Denmark; stipp@nano.ku.dk
* Correspondence: balogh_brunz@hartwick.edu; Tel.: +1-607-431-4734

Received: 7 June 2017; Accepted: 15 September 2017; Published: 19 September 2017

Abstract: Ectomycorrhizal fungi and associated bacteria play a key role in plant-driven mineral weathering and uptake of mineral-derived nutrients in the rhizosphere. The goal of this study was to investigate the physical and chemical characteristics of bacteria-fungi-mineral interactions in biofilms of Scots and red pine rhizospheres. In three experiments, seedlings were grown in columns containing silica sand amended with biotite and calcium-feldspar, and inoculated with pure cultures of ectomycorrhizal fungi or a soil slurry. Uninoculated seedlings and unplanted abiotic columns served as controls. After nine months, the columns were destructively sampled and the minerals were analyzed using scanning electron and atomic force microscopy. Element release rates were determined from cation concentrations of input and output waters, soil exchange sites, and plant biomass, then normalized to geometric surface area of minerals in each column. The results revealed that various ectomycorrhizal fungal species stimulate silicate dissolution, and biofilm formation occurred at low levels, but direct surface attachment and etching by fungal hyphae was a minor contributor to the overall cation release from the minerals in comparison to other environmental conditions such as water applications (rain events), which varied among the experiments. This research highlights the importance of experimental design details for future exploration of these relationships.

Keywords: cation limitations; mineral weathering; scanning electron microscopy; atomic force microscopy; column experiments; *Pinus resinosa*; *Pinus sylvestris*; ectomycorrhizal fungi

1. Introduction

Silicate mineral weathering is important to many element cycles, soil formation, and nutrient supplies for plants and ecosystems, and is key to long-term carbon dioxide sequestration in the Earth's system [1–3]. In soil environments, plant roots and their associated fungi and bacteria are increasingly recognized as the main drivers of silicate weathering both in natural [4–11] and in agricultural settings [12–14]. The rhizosphere (root influenced zone) has been described as the most important and most active part of the critical zone (CZ) [15,16], which is defined as "the heterogeneous, near-surface environment in which complex interactions involving rock, soil, water, air, and living organisms regulate the natural habitat and determine the availability of life-sustaining resources" [17]. It is well established that both ecto- and endo- mycorrhizal fungi enhance mineral weathering and improve the

nutritional state of higher plants [18–20]. Some studies have demonstrated that ectomycorrhizal fungi are able to find hotspots of mineral sources of cation nutrients [21,22], and dissolve the minerals to obtain the needed nutrients [20,23–27]. In systems with low base cation availability, mycorrhizal fungi and their bacterial helpers significantly increased weathering rates and decreased the loss of weathering products [9,28–31]. Indeed, several studies have documented chemical and physical alteration of biotite (and other sheet silicates) as the result of direct fungal attachment to these mineral surfaces [30,32–36]. While these mechanisms clearly can increase the capacities of plants and ecosystems to acquire nutrients under certain conditions, some researchers are skeptical of the significance of rhizospheric microbial contributions to weathering budgets of real ecosystems and watersheds [37–41]. Part of the problem is that the effective definition of weathering used in a given study inevitably depends on the scale and the technique of investigation [31,42,43]. Rapid weathering acquisition of nutrients by a plant or plant community does not necessarily generate pools of weathering products in soils, soil waters, or runoff from catchments where weathering estimates are often made [44,45]. A related issue, revealed by modeling, is related to time scale—for example, over geological time where net changes in ecosystems are small relative to total weathering fluxes, weathering rates depend on factors exogenous to the ecosystem, such as volcanic CO_2 input rate to the atmosphere [1,46]. An interesting question under debate is whether soil water mediates and can be monitored to quantify weathering mass transfers [7,37], or if plant uptake in particular might involve some mechanism of contact exchange directly between ectomycorrhizal fungi (EMF) and mineral surfaces. [4,20–22,30,32–36].

Laboratory, mesh bag, soil profile, watershed, and modeling studies of the roles of plants and associated fungi and bacteria on weathering, nutrient uptake, and soil formation have generated a broad range and variety of results. These variations suggest that other factors, not monitored or controlled in the studies, might have crucial roles [47]. Such factors could be water usage and availability, rooting depth, species specificity of associated fungi and bacteria, varying plant adaptation strategies, and the complexity of interacting factors in natural systems [47,48]. Thus, quantification and relative contributions of the processes and players are still problematic.

Our previous studies and the published results of others indicate that the formation of rhizospheric biofilms on soil mineral surfaces in collaboration between plant roots, mycorrhizal fungi, and associated bacteria suggest an important regulatory mechanism to increase chemical weathering and decrease chemical denudation (loss) at the same time [30,45,46]. Our goal was to investigate the physical and chemical characteristics of bacteria-fungi-mineral interactions under biofilm covers in the rhizosphere of selected pine species. We aimed to test (i) the response of biofilm development of various fungi and their bacterial associates in the rhizosphere of Scots (*Pinus sylvestris* L.) and red pine (*Pinus resinosa* Ait.) to cation nutrient limitation, as well as (ii) the rates of mineral dissolution of the various biological combinations under cation nutrient limitations. Figure 1 graphically summarizes our weathering "undercover" hypotheses that: (i) rhizospheric biofilm development is enhanced at the bacteria-fungi-mineral interface under base cation limitations, and (ii) the rhizospheric biofilm, which incorporates both bacteria and fungi, facilitates increased uptake of base cation nutrients into seedling biomass by localizing and concentrating the weathering products of the minerals.

Results from three column experiments are presented in this paper. A new experiment (KU), conducted with Scots pine was inoculated with pure cultures of three ectomycorrhizal fungal species. We also present previously unpublished results from a study [49] conducted with red pine inoculated with a soil slurry (ZS) and from dissertation research [50], where red pine was inoculated with pure cultures of ectomycorrhizal fungi and bacteria associated with those fungi (BB) [30].

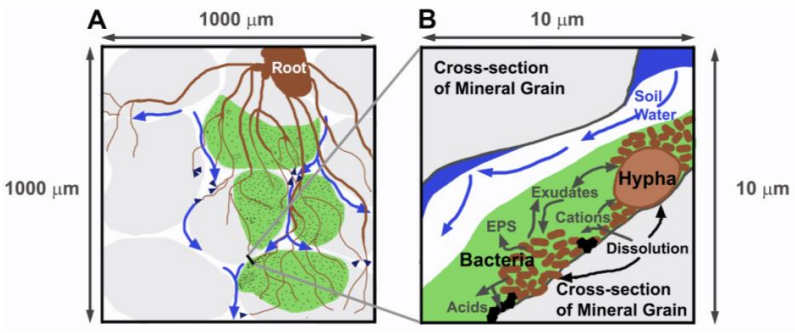

Figure 1. Conceptual model of the hypothesized biofilm weathering reactor in the rhizosphere. (**A**) Soil mineral particles shown in light gray; soil water movement by gravity shown by blue arrows; green (darker gray) shaded regions are patches of biofilm covering mineral surfaces, with brown stipples indicating embedded bacteria. Fine lines represent fungal hyphae that have grown into the pore network, attached to mineral surfaces, embedded in biofilm patches, and connected to the root. Small dark arrows show soil water uptake by fungal hyphae; (**B**) Cross-section through an unsaturated pore and two mineral grains, showing fungal hypha and bacteria embedded in biofilm attached to a mineral surface. Dissolution, uptake of cations, and precipitation of secondary minerals (black diamonds) are indicated along the biofilm-hypha-bacteria-mineral interface. Acids, various exudates, extracellular polymeric substances (EPS) are released into biofilm, which facilitates the interaction among bacteria, fungi, and mineral surfaces, and isolates the covered surface from resident soil water that flows (blue arrows) episodically during infiltration events.

2. Materials and Methods

The experiment with Scots pine, which was conducted at University of Copenhagen in Denmark and is designated as KU, is described in detail in this manuscript. The other two experiments with red pine, which were conducted at Washington State University, are described in Shi et al. [49] for the experiment designated as ZS, and in Balogh-Brunstad et al. [30] for the experiment designated as BB. Here, only a brief description is provided for these last two experiments, emphasizing the methods that were not previously described and pointing out similarities and differences among the experiments. Treatment codes are defined in Table 1.

Table 1. Treatment codes and description of treatments used in this paper. KU = University of Copenhagen experiment, ZS = experiment described in Shi et al. [49], BB = experiment described in Balogh-Brunstad et al. [30].

Experiment	Treatment Codes	Description
KU	KU_A	Abiotic (A) unplanted treatment
	SP_UI	Scots pine (SP) uninoculated (UI)
	SP_SB	Scots pine inoculated with *Suillus bovinus* (SB)
	SP_PF	Scots pine inoculated with *Piloderma fallax* (PF)
	SP_PI	Scots pine inoculated with *Paxillus involutus* (PI)
ZS [49]	ZS_A	Abiotic unplanted treatment
	RP_UI	Red pine (RP) uninoculated (UI)
	RP_SS	Red pine inoculated with soil slurry (SS)
BB [30]	BB_A	Abiotic unplanted treatment, both antibiotics and fungicides are used to prevent growth the bacteria and fungi.
	RP_E	Red pine inoculated with *Ewingella americana* (E), which was isolated from the *Suillus tomentosus* sporocarps, and fungal growth was prevented by fungicides.
	RP_BP	Red pine inoculated with *Bacillus megaterium* (B) and *Pantoea agglomerans* (P), which were isolated from the *Pisolithus tinctorius* sporocarps, and fungal growth was prevented by fungicides.
	RP_ST_E	Red pine inoculated with *Suillus tomentosus* (ST) and its associated bacterium, *Ewingella americana*
	RP_PT_BP	Red pine inoculated with *Pisoluthus tinctorius* (PT) and its associated bacteria, *Bacillus megaterium* and *Pantoea agglomerans*

2.1. Seed Germination and Inoculation

The KU experiment was started by germinating seeds of Scots pine (from the Botanical Gardens of the Natural History Museum of Denmark, Copenhagen, Denmark) on 1.5% H_2O agar after sterilization with 30% H_2O_2. After germination, 45 of the most vigorous seedlings of Scots pine were inoculated with one of the pure cultures of the three ectomycorrhizal fungi (15 each) obtained from the Swedish University of Agricultural Sciences, Uppsala, Sweden: *Paxillus involutus* (PI), *Suillus bovinus* (SB), and *Piloderma fallax* (PF). These fungi were selected because they are commonly found in natural Scots pine forests and they have been grown successfully under laboratory conditions [20,24,41,51–54]. Scots pine inoculation was carried out at Lund University, Sweden, on a peat-vermiculite and MMN (Marx-Melin-Norkrans) sterilized medium in a volume ratio of 1:5:3 [55] (Table S1) in round, sealed Petri dishes with the seedlings protruding through a notch cut into the Petri dish. The notch was sealed with sterilized lanolin. The Petri dishes were then placed into a growth cabinet (16/8 h, 18/16 °C day/night around 300 µmol PAR—photosynthetically active radiation) in an upright position, keeping the roots and fungi in the dark for about eight weeks to allow the fungi to colonize the roots [51]. The remaining 15 vigorous seedlings were kept as uninoculated controls grown under the same conditions. After eight weeks of growth, the root systems of each seedling were examined using a reflected light, dissecting microscope, through the clear wall of the Petri dishes for signs of ectomycorrhizal associations and contamination. Contamination was found in two seedlings, which were discarded. Then, 10 Scots pine seedlings of each treatment with the most visible mycorrhizal root tips on their root systems were selected for transplanting to growth tubes. Ten of the healthiest, uninoculated seedlings were selected for the experiment as controls.

The ZS experiment was set up simultaneously with the KU experiment. Red pine seeds were obtained from Sheffield's Seed Co, Inc., Locke, NY, USA and sterilized with 35% H_2O_2. Seed germination and seedling growth were carried out the same way as described in the KU experiment but without initial inoculation [49]. After about three months of growth, the seedlings were transplanted into growth cells and inoculation with soil slurry was carried out there. The inoculum preparation is described in detail in Shi et al. [49]. Briefly, inoculum was prepared from soils and roots collected from the root zone of young Western white pines at 20 miles northeast of Potlatch, ID [49], which is the same location that provided the sporocarps for the BB experiment [30]. The soil and roots were suspended in 500 mL of deionized and sterile water, filtered with a Whatman No. 1 paper filter, then 20 mL of this soil slurry was added to half of the seedlings. Thirty replicates were prepared for each treatment with seedlings.

The BB experiment differed in its seed germination (details in [30]). Five red pine seeds were directly sown into the columns after sterilization with 30% H_2O_2. After one month growth, the seedlings were thinned to one per column and, after allowing an additional month of root development, the seedlings were inoculated with a suspension of pure culture of *Suillus tomentosus* (ST), or *Pisolithus tinctorius* (PT) fungi, and/or with pure cultures of *Ewingella americana* (E), and/or a combination of *Bacillus megaterium* (B) and *Pantoea agglomerans* (P) bacteria, which were isolated from ST and PT respectively [30]. Each treatment was replicated 15 times.

2.2. Experimental Setup

The Scots pine seedlings in the KU experiment were transplanted into 164-mL opaque UV blocking plastic SC-10 Ray Leach tubes (3.8-cm inside diameter, 21-cm depth, Stuewe and Sons. Inc., Tangent, OR, USA) filled with acid-washed white quartz sand (98.8% SiO_2, 0.63% Al_2O_3, 0.36% K_2O; Dana Kvarts, Danks Kvarts Industry, Brædstrup, Denmark) amended with 1 wt % biotite ($(Ca_{0.27}, K_{1.75})(Mg_{2.66},Fe_{2.28},Al_{0.69},Ti_{0.37})(Si_{5.67},Al_{1.85})O_{20}(OH)_2$), and 1 wt % calcium-rich plagioclase feldspar ($(Ca_{2.57},Na_{1.14},K_{0.07})(Al_{5.29},Fe_{0.79})Si_{10.05}O_{32}$). These minerals were the sole sources of potassium and calcium in the growth experiment. They were obtained from Dr. F. Krantz Rheinisches Mineralien-Kontor GmbH & Co. KG, Bonn, Germany and the composition was determined using X-ray fluorescence (XRF) elemental analysis at the Geoanalytical Lab of WSU, Pullman, WA, USA [56,57].

The quartz sand was soaked in 10 vol % hydrochloric acid for 24 h, well mixed every 6 h, then rinsed with deionized water until the pH of the rinse water reached 6, after which it was dried in an oven at 90 °C. The amendment minerals were crushed, sieved, washed in deionized water, and dried at 90 °C, then a particle size range of 125–500 μm was selected. The sand and minerals were mixed and placed into each column. Then, before the seedlings were transplanted into them, they were leached with deionized water for two weeks to reduce the effect of freshly disturbed and broken mineral surfaces. Unplanted abiotic controls (KU_A) were also prepared, in addition to uninoculated controls (SP_UI) and the three fungal treatments (SP_SB, SP_PF, and SP_PI) in replicates of 10 each (Table 1). Time zero for start of the column experiment was defined when the colonized seedlings were transplanted into the sand-mineral growth medium. All columns were placed in a growth chamber under 16/8 h, 18/16 °C day/night, around 50–80% humidity, and 300 μmol PAR. The seedlings were subjected to cation (calcium and potassium) nutrient limitation by providing them with 10 mL of sterilized deionized water twice a week and 10 mL of calcium- and potassium-free nutrient solution once a week (composition is listed in Table S2). Fungicides (pH 5.5; 0.5 ppm Ca, 0.1 ppm Mg), Steptomycin sulfate (100 μg/mL), and Nystatin (40 μg/mL; Sigma Chemical Company, St. Louis, MO, USA) were applied to KU_A and SP_UI treatments, at a dose of 1 mL once every two months to prevent fungal growth [30]. Bacterial growth was not prevented after the start of the experiment in any of the treatments, i.e., antibiotics were not supplied. A rain event with an application of 50 mL deionized water was simulated after zero, three, six, and nine months of growth to collect gravity-drained water from the columns for chemical analysis. The water applied during the experiment was equivalent to 150 cm per year precipitation.

The red pine seedlings in the ZS experiment were transplanted into the same type of SC-10 Ray Leach tubes as the seedlings of the KU experiment, containing acid-washed silica sand (98.6% SiO_2, 0.78% Al_2O_3, 0.21% K_2O; Lane Mountain Company, Valley, WA, USA) amended with 0.5 wt % biotite ($(Ca_{0.16},K_{1.53})(Mg_{2.89},Fe_{2.34},Al_{0.53},Ti_{0.24})(Si_{6.16},Al_{1.37})O_{20}(OH)_2$) and 1 wt % anorthite ($(Ca_{2.50},Na_{1.29},K_{0.19})(Al_{5.93},Fe_{0.57})Si_{9.98}O_{32}$) (WARD's, Rochester, NY, USA). The sand and mineral preparations and the experimental growth conditions were identical to the KU experiment, as described above and in Shi et al. [49]. The description of the composition of the calcium- and potassium-free nutrient solution and the irrigation regime of the experiment is presented in Shi et al. [49], similar to the KU experiment with a rainfall equivalent of 80 cm per year. Time zero for the start of the column experiment was defined as the time when the seedlings were inoculated. While this experiment aimed to study the contribution of soil bacteria and fungi to silicate mineral weathering under various calcium and potassium availabilities, the slurry inoculation method did not work well and ectomycorrhizal fungal colonization was unsuccessful [49]. In this paper, the composition and microscopy (previously unpublished) results of the calcium- and potassium-free nutrient treatments of the red pine seedling only (RP_UI), the red pine with soil slurry inoculation (RP_SS), and the unplanted abiotic controls (ZS_A) are compared with the results from the KU experiment (Table 1).

Results from the BB experiment [30] are also used for comparison, where ectomycorrhizal colonization of red pine was established through pure culture inoculation. Red pine seedlings were grown in the same type of SC-10 Ray Leach tubes as in the studies described above, that used acid-washed silica sand (Lane Mountain Company, Valley, WA, USA) amended with 1.5 wt % biotite and 3 wt % anorthite (WARD's, Rochester, NY, USA). The composition and preparation of the minerals are described in Balogh-Brunstad et al. [30]. An unplanted abiotic treatment (BB_A) served as the control for the four biotic treatments described in Table 1. The growth conditions of the BB experiment were identical to the other two experiments described above, and a detailed explanation is found in Balogh-Brunstad et al. [30]. Through irrigation, the columns received an annual rain equivalent of 250 cm per year.

After nine months, in each experiment the columns were destructively sampled for determining bulk weathering rates and for microscopic analysis. The seedlings were harvested by gently rolling the growth columns to loosen the connection between the tube and the material inside and then

the seedling, with its intact soil core, was lifted out and placed on a clean surface. The seedling was separated from the soil, carefully keeping the root system intact. Particles adhered to the roots were shaken off as much as possible, then the remaining particles were washed off using deionized water. The shaken-off plus washed-off particles were defined as the "rhizospheric soil" in each experiment. Then, each entire root system was documented by scanning at high resolution on a flatbed scanner, or high-resolution photographs of the root system were taken. Mycorrhizal root tips were counted on these images, and the percentage of mycorrhizal root tips was determined for each seedling. In addition, seedlings were randomly selected from each treatment and those roots were examined using a dissecting microscope to verify the counts obtained from the images. In both cases, the ectomycorrhizal root tips were selected based on the assumption that roots with typical ectomycorrhizal morphology and anatomy are mycorrhizal [58].

2.3. Chemical Analysis

In all experiments, bulk weathering rates of biotite and calcium-rich plagioclase feldspar were estimated by measuring calcium and potassium mass partitioned from the minerals into other phases [30]. Irrigation water, drainage water, and biomass were analyzed for calcium and potassium concentration. The biomass was separated for above- and below-ground parts, oven dried at 65 °C until the mass remained unchanged, then milled and wet digested with concentrated nitric acid and 30% H_2O_2 [59]. The digests were dried, then reconstituted in 1% nitric acid. Exchangeable cation concentrations of the sand-mineral growth medium were determined using an ammonium acetate extraction procedure [60]. All liquids were analyzed using atomic absorption spectroscopy (AAS; AAnalyst 600, PerkinElmer, Waltham, MA, USA) at the Nano-Science Center, University of Copenhagen and concentrations in the samples were determined using a set of diluted certified standards. Shi et al. [49] used the same sample preparation and the aliquots were analyzed for calcium on an inductively coupled plasma – mass spectrometry (ICP-MS; (Agilent 7700x, Agilent Technologies, Santa Clara, CA, USA)) and for potassium on an AAS (Varian SpectrAA 220, Varian, Palo Alto, CA, USA) at Washington State University (WSU). Balogh-Brunstad et al. [30] also used the above sample collection and preparation and the aliquots were analyzed on an inductively coupled plasma – optical emission spectrometry (ICP-OES;model 61, Thermo Jarrell Ash Corporation, Franklin, MA, USA) at WSU.

Weathering rates were expressed as element release rates, determined for each treatment in each experiment in mmol/m^2 of mineral surfaces [61,62]. The total amounts of calcium and potassium were calculated in irrigation and drainage waters, biomass, and soil exchange sites; then, the total release was determined by a simple mass balance of output minus input for all pools [30].

$$\textit{Total Element Release} = \textit{(Change in Biomass)} + \textit{(Drainage} - \textit{Irrigation water)} + \textit{(Change in Exchangeable Cation Pool of Growth Medium)}$$

The total element release was divided by the estimated geometric surface area of the source mineral grains (in m^2). The geometric surface area of the minerals was estimated based on the particle size range, shape, added mass, and density of the minerals (Table S3). Normalization of the total release by the geometric surface area of the mineral in each column allowed comparison of different treatments assuming that all of the calcium was released from the feldspar and all of the potassium was released from the biotite. Although normalizing the results to the geometric surface area instead of the measured effective surface area of the mineral particles is not ideal, it allows comparison among the treatments because the minerals were processed the same way, the particle size range was about the same, and the experiments were run for the same time length [30,49].

The biotic enhancement ratio for each element is defined as the total element release rate in a given biotic treatment divided by the total release rate of the abiotic treatment in that experiment.

All calculations were completed on three to five replicates of each treatment. Data analysis was carried out in Microsoft Excel, using the data analytical package. Differences among treatments

within each experiment were determined by one-way ANOVA analysis. When the p value was lower than 0.05, then a least significant difference t test (LSD) post hoc test was carried out to determine which pairs of treatments were significantly different from each other among the various treatments. The experiments were also compared to each other using the same methods, but cross-experiment comparison results were treated cautiously, because these experiments had few replicates, small sample size, high variability, and the effects of host, fungal species, and water availability variations could not be tested in these experimental setups.

2.4. Atomic Force Microscopy (AFM) Analysis

In the KU experiment, AFM was used to obtain high resolution images of biotite surface topography at the nanometer scale. Samples were prepared with minimal alteration. As the columns were destructively sampled, the seedlings were carefully removed, the rhizospheric soil was homogenized, and a subsample was taken for AFM analysis before the soil was set to dry. Freshly sampled biotite and feldspar grains were mounted on a glass microscopy slide using a double-sided adhesive tape and imaged with AFM (Asylum Research AFM-3D-SA, Oxford Instruments Company, Santa Barbara, CA, USA) at the Nano-Science Center, University of Copenhagen, Copenhagen, Denmark). The samples were imaged using tapping mode in air, at room temperature, with 0.5 to 1 Hz scanning rate. Images were analyzed and processed with Igor Pro 6.03A.

2.5. Scanning Electron Microscopy (SEM) Analysis

To obtain a better understanding of the overall surface morphology of the components of the rhizosphere, the samples were imaged using SEM at the site where the experiments were done. All of the KU samples were processed and imaged using an FEI Quanta 3D field emission gun (FEG) SEM (FEI Company, Hillsboro, OR, USA) at the Nano-Science Center, University of Copenhagen, Denmark. The samples were imaged using a secondary electron (SE) detector in variable pressure mode, uncoated, at 5 kV accelerating voltage, with a ~5-mm working distance and without tilt. The ZS samples were imaged using an SE detector on an FEI Helios Nanolab dual-beam focused ion beam/SEM (FEI Company, Hillsboro, OR, USA) at the Environmental Molecular Sciences Laboratory, the Pacific Northwest National Laboratory, Richland, WA, USA and on a JEOL JSM636OLV SEM (JEOL Ltd., Tokyo, Japan) at the Department of Geology, Colgate University, Hamilton, NY, USA. These samples were carbon-coated (Cressington Carbon coater 108 carbon/A; Cressington Scientific Instruments, Watford, UK) before imaging to decrease charging. The nine-month samples of the BB experiment were also imaged using an SE detector on a Zeiss Leo 982 field emission SEM (Carl Zeiss Ag, Oberkochen, Germany) at Pacific Northwest National Laboratory, Environmental Microbiological Science Laboratory, Richland, WA, USA [30].

Sample preparation for the SEM investigations was done in the same way for each experiment. After destructive sampling of the columns, the rhizospheric soil was air dried separately from the rest of the soil and subsampled for microscopic analysis. Hand-separated biotite and feldspar grains were mounted on carbon tape-covered aluminum SEM stubs (Ted Pella, Redding, CA, USA), and sputter-coated with carbon for the ZS experiment, and examined uncoated for the KU experiment. To generate a representative characterization of each treatment, three replicate SEM stubs were prepared with a minimum of five grains of each mineral from each treatment, then the mineral grains were imaged at 10 random locations under very similar resolution among the various SEMs. Thus for each treatment, a minimum of 30 images of biotite were examined for signs of fungal weathering, which were defined as features of fungal hyphae size (2 to 5 μm in diameter in these experiments), as well as curved and branching channel shaped features. The area percentage of these fungal features was compared to the total biotite area imaged, which provides a semi-quantitative estimate of the direct surface alteration caused by fungal hyphae, from which standard error was determined for the replicated samples [30,32,33]. Fungal etching on the calcium-rich feldspar grains could not be quantified because of the initial roughness of the grains.

3. Results

3.1. Bulk Composition

After nine months' growth, the seedlings in the three experiments were significantly different in size ($p < 0.001$). Scots pine seedlings grew very slowly both above- and below-ground (Table 2). All seedlings of the SP_UI treatment died by month 5, where the seedlings were grown without mycorrhizal inoculation, thus no results of this treatment are shown. In contrast, the red pine seedlings in ZS and BB experiments with and without inoculation became root-bound as the roots explored the whole soil volume and filled the growth tubes entirely. The seedlings produced three to 10 times more above-ground biomass than the Scots pine seedlings (Table 2). However, the root:shoot ratios of dry biomass weight were the same for the KU and the ZS experiments and substantially larger for the BB experiment (Table 2).

Table 2. Above- and below-ground biomass in mg after nine months' growth, the root:shoot ratios, and the mycorrhizal root tip percentage of the root system are shown for each column experiment; the BB treatments are recalculated from Balogh [50]. Standard deviation of four to five replicates of each treatment is shown in parenthesis; a–d (the different superscript letters) within each column indicate statistically significant differences among the treatments (Table S5). Treatment codes are defined in Table 1.

Experiment	Treatment Codes	Above-Ground Biomass (mg)	Below-Ground Biomass (mg)	Root:Shoot Ratio	% of Mycorrhizal Root Tips
KU	SP_SB	20.3 (±2.4) ^{a}	7.13 (±2.8) ^{a}	0.37 (±0.2) ^{a}	54 (±17) ^{a}
	SP_PF	27.0 (±4.4) ^{a}	13.1 (±4.9) ^{a}	0.48 (±0.1) ^{a}	67 (±15) ^{a}
	SP_PI	28.8 (±6.3) ^{a}	24.0 (±11) ^{b}	0.82 (±0.3) ^{a}	53 (±19) ^{a}
ZS [49]	RP_UI	209 (±120) ^{b}	73.0 (±46) ^{c}	0.35 (±0.1) ^{a}	0.0 (±0) ^{b}
	RP_SS	242 (±170) ^{b}	61.2 (±18) ^{c}	0.35 (±0.2) ^{a}	2.1 (±2) ^{b}
BB [30,50]	RP_E	116 (±30) ^{a}	288 (±80) ^{d}	2.49 (±0.36) ^{b}	0.0 (±0) ^{b}
	RP_BP	106 (±34) ^{a}	280 (±75) ^{d}	2.74 (±0.63) ^{b}	0.0 (±0) ^{b}
	RP_ST_E	92.6 (±23) ^{a}	218 (±39) ^{d}	2.39 (±0.35) ^{b}	22 (±5) ^{c}
	RP_PT_BP	105 (±16) ^{a}	276 (±65) ^{d}	2.62 (±0.36) ^{b}	5.3 (±0.4) ^{d}

Potassium release in the KU experiment was similar to that in the BB experiment, but the ZS experiment had significantly lower potassium release ($p < 0.001$; Figure 2A; Table S4). Variation was large between replicates and was independent of fungal species within the experiments. Calcium release was significantly higher in the KU columns with Scots pine compared to that in the ZS columns and BB columns with red pine ($p < 0.001$; Figure 2B; Table S4). Biotic enhancement ratios show an observable difference between the Scots pine and red pine experiments for potassium ($p < 0.001$) and no difference for calcium ($p = 0.08$; Figure 2C). The pH of the drainage waters was similar in both the KU and the ZS experiments; at the start of the experiments it was close to neutral (~6.00 to 6.80). The pH of the abiotic treatments remained around 6.00 in both experiments and the treatments with all of the seedlings and added microbes/fungi dropped to acidic levels (~3.60 to 4.50) by the end of the sixth week and remained acidic for the remainder of the experiments [49]. The pH stayed circumneutral in the BB experiment [30].

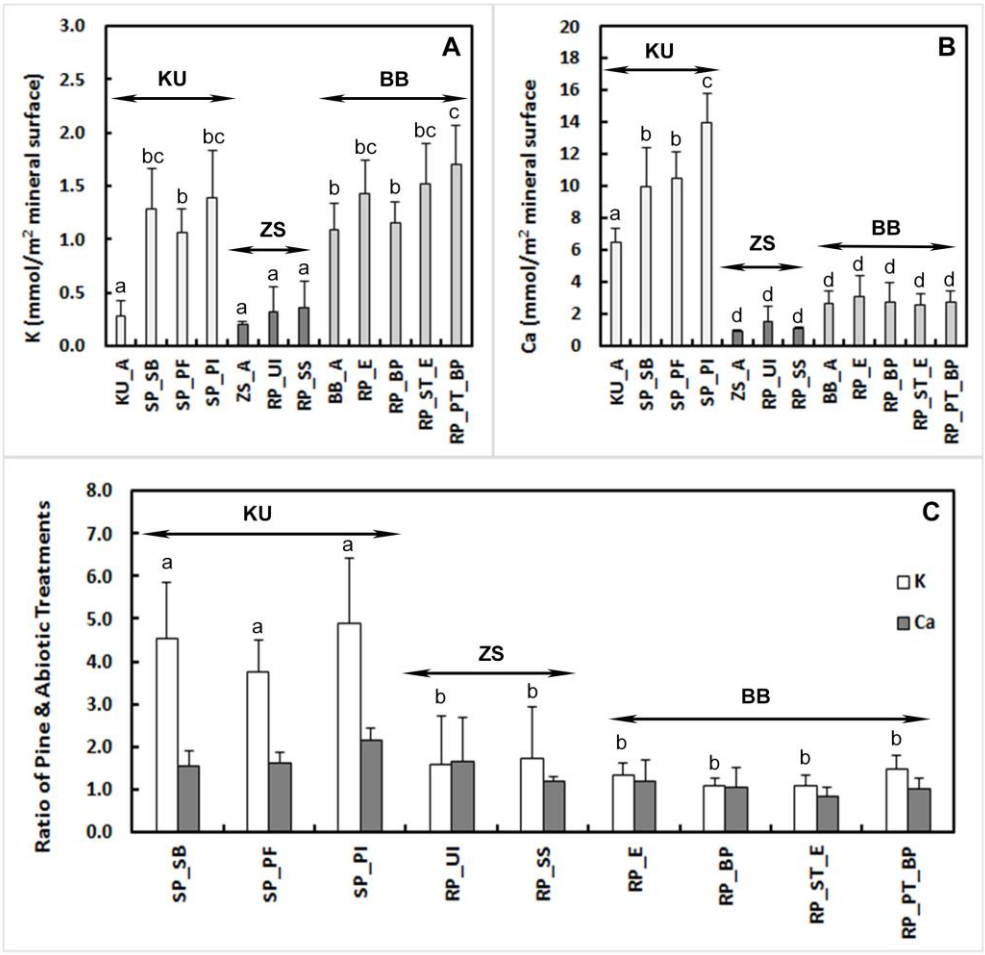

Figure 2. Element release of potassium (**A**) and calcium (**B**) in mmol per m^2 of geometric surface area of the minerals. Biotic enhancement ratio is shown by the element release of treatments with pine seedlings normalized to the element release of abiotic treatments (**C**). Error bars represent the standard deviation of three to four replicates. The lower case letters (a–d) within each panel represent statistically significant differences among the treatments (Table S5). In panel (**C**), the calcium ratios did not have statistical difference, thus no letters are presented.

3.2. Mineral Surface Analysis

3.2.1. Atomic Force Microscopy (AFM)

In the KU experiment, after nine months of exposure to the rhizosphere of the three pine treatments, biotite exhibited shallow etched channels in all treatments (Figure 3A–C), while the samples from the abiotic treatment remained nearly unchanged (Figure 3D). The shallow channels observed on the biotite flakes are about 10 nm deep, and thus not observable by SEM. Based on size, shape, and distribution, we interpret that they are fungus-generated (Figure 4A). Feldspar surfaces were harder to evaluate, because the original surfaces had steps and high roughness, but the roughness increased and etch pits were also detected (Figure 4B) Biological colonization of the mineral surfaces was patchy and highly variable. Thick biofilm did not develop, but layers of extracellular polymeric substances (EPS) were the dominant biological markers on SP_PI (Figure 5A); bacteria and fungi dominated the surfaces on SP_PF (Figure 5B); and SP_SB was almost free of biological material (Figure 5C). KU_A remained much smoother, with neither channels nor biological material evident (Figure 5D).

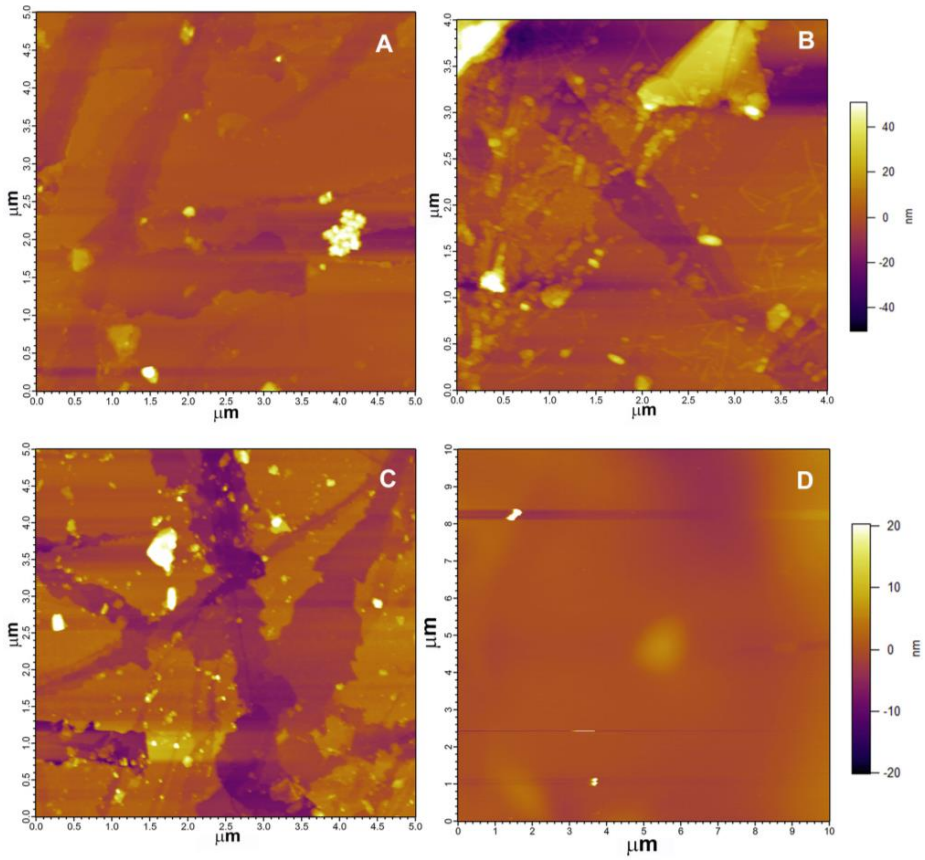

Figure 3. Atomic force microscopy topography images of biotite surfaces in the KU experiment for SP_PI (**A**); SP_PF (**B**); SP_SB (**C**); and KU_A (**D**). Images (**A**)–(**C**) show shallow 7- to 20-nm-deep etched fungal hyphae size channels while the abiotic surface (**D**) remained unchanged. The colored bars on the right side of the images show the z-scale for the two images in each row.

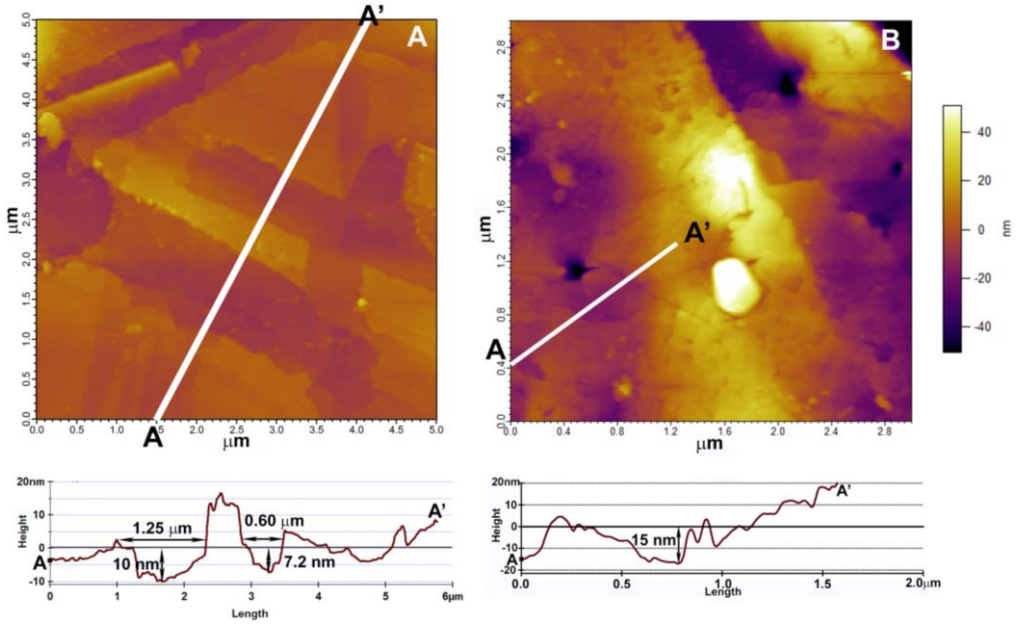

Figure 4. Atomic force microscopy topography images from the KU experiment showing the dimensions of shallow channels on a biotite surface (**A**) and etch marks on a feldspar surface (**B**) along the A–A′ lines; examples from SP_PI treatment. The colored bar on the right shows the z-scale.

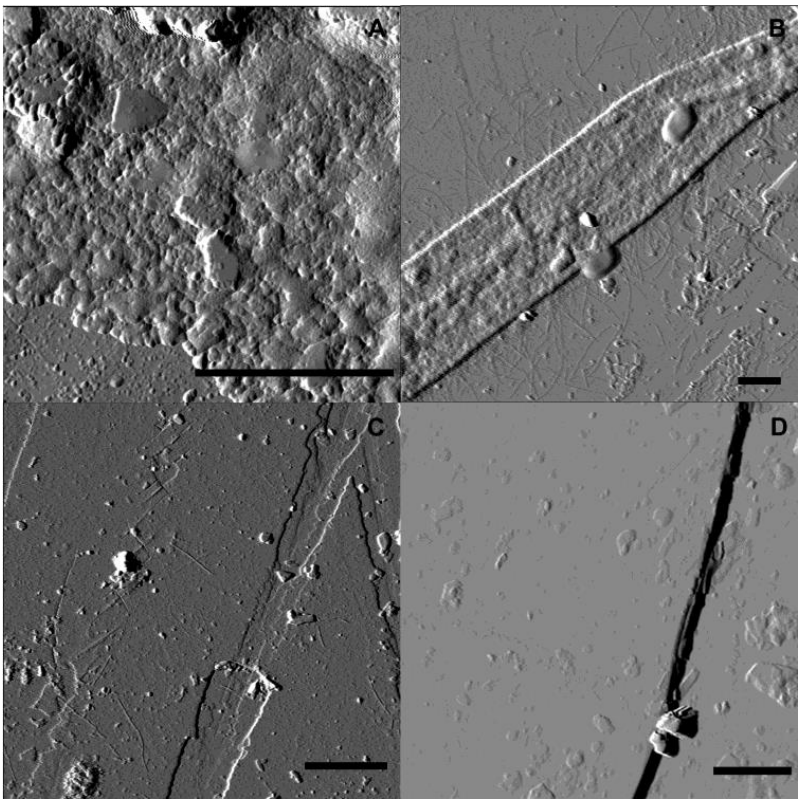

Figure 5. Atomic force microscopy amplitude retrace (deflection) images from the KU experiment showing the shape of the surface-covering materials (here, z-scale is irrelevant). The black bar represents 1 µm horizontal distance on all images. Extracellular polymeric substances (EPS) biolayers are dominant on biotite surfaces of SP_PI (**A**); fungal hyphae and bacteria are attached to most of the biotite surfaces of SP_PF (**B**); and almost no biological material is found on the biotite surfaces of SP_SB (**C**); lastly, biotite surfaces are relatively clean in the abiotic KU_A treatment (**D**).

3.2.2. Scanning Electron Microscopy (SEM)

The SEM images showed differences in the rhizospheric environments of the treatments. The successful fungal colonization of red pine roots in the BB experiments showed the most prominent fungal hyphal attachment (Figure 6A) and biofilm formation (Figure 6B) on the biotite surfaces. While the roots of the seedlings of the KU experiment were well colonized with one of the three ectomycorrhizal fungi, the attachment of hyphae to biotite surfaces was less prominent (Figure 6C), but large amounts of organic exudates were associated with these fungal species (Figure 6D,E). In the ZS experiment, where the inoculation was made nonspecifically using a soil slurry, fungal colonization was insignificant; however, root hairs were found to be attached to biotite surfaces (Figure 6F). Overall, biological markers were patchily distributed on the mineral surfaces in all of the experiments and biotite was favored over feldspar.

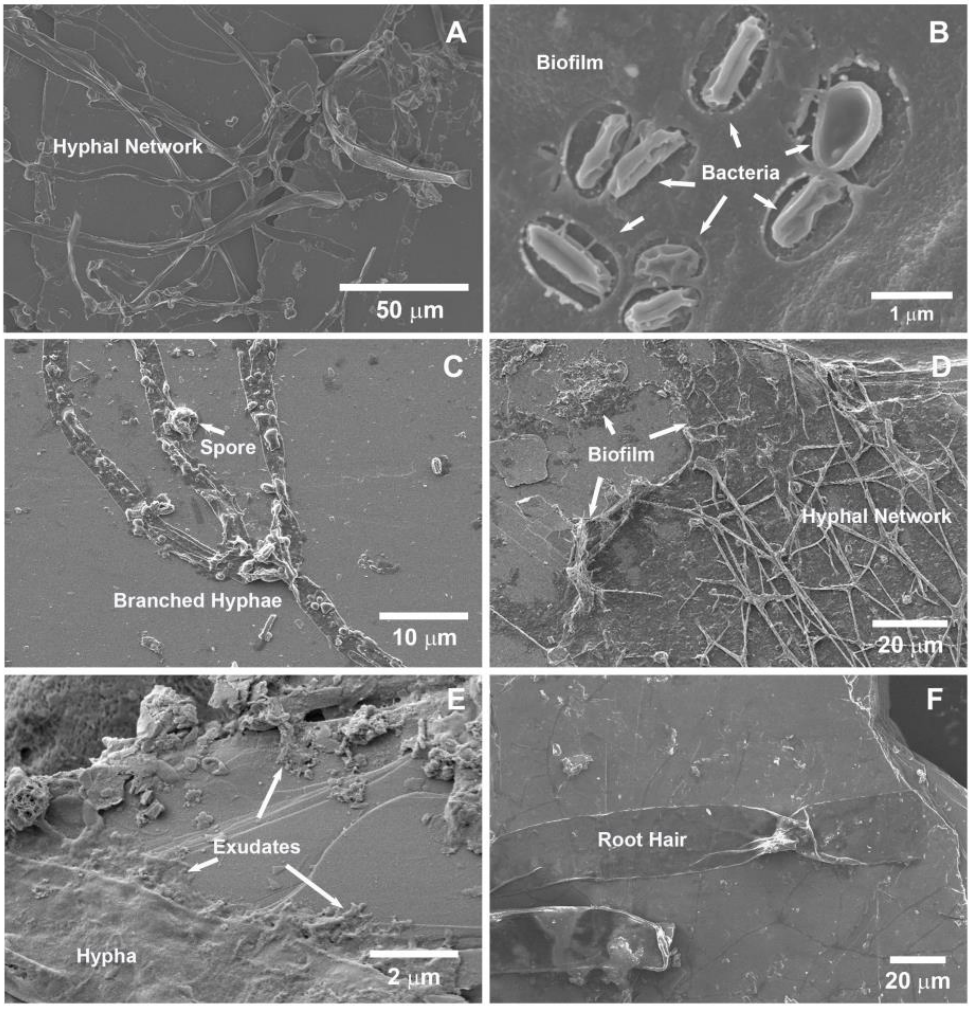

Figure 6. Scanning electron microscopy images of the rhizosphere biotite surfaces of various treatments. Abundant fungal hyphal attachment is seen in RP_ST_E (**A**) and biofilm formation with desiccated bacteria in RP_E (**B**); Some desiccated fungal hyphae are observed in SP_PI (**C**); fungal hyphae with a large amount of organic exudates are seen in SP_SB (**D**); and organic exudates along the edge of the hyphae are seen in SP_PI (**E**); finally, the sample from the RP_SS treatment only exhibited root hairs on the biotite surfaces (**F**). Treatment codes are defined in Table 1.

In addition to the bulk composition data, evidence of mineral dissolution is shown by channel-like etching patterns on the biotite surfaces in all pine treatments. These are either fungal hyphae size (Figure 7A) or root hair size (Figure 7B). Secondary mineral precipitates are also seen on the mineral grain surfaces, especially accumulated on the feldspar surfaces (Figure 7C,D). While the abiotic treatments exhibit some secondary precipitates, the mineral grain surfaces remain smoother and show no biological etching features (Figure 7E,F). Semi-quantitative estimates of area coverage of fungal hyphae-produced channels are the greatest in the RP_PT_BP (11%) and RP_ST_E (21%) of the BB experiment, and lower in the SP_PF (9%), SP_PI (4%), and SP_SB (1%) of the KU experiment. Larger sized (root hair) channel-like features (Figure 7B) covered the biotite surfaces in RP_E (15%), RP_BP (8%), RP_SS (23%), and RP_UI (2%).

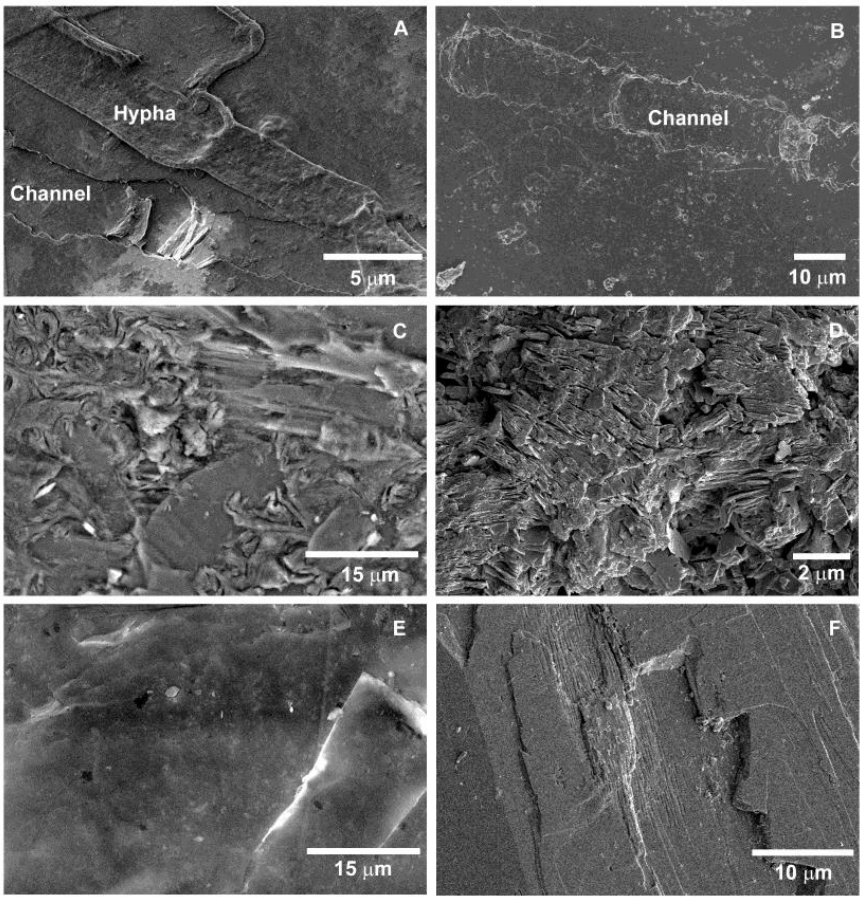

Figure 7. Scanning electron microscopy images of the rhizosphere mineral surfaces from various treatments. Fungal hypha-sized channels were found on biotite in most treatments with fungi, for example, from SP_PI (**A**); pine treatments without fungi have root hair-diameter channels, example from RP_BP (**B**); Secondary mineral precipitates were best exhibited on the feldspar grains, as seen in the RP_SS (**C**) and SP_SB (**D**) treatments. The abiotic samples remained relatively smooth and without biological etching marks, as shown by the biotite example from ZS_A (**E**) and a feldspar example from KU_A (**F**). Treatment codes are defined in Table 1.

4. Discussion

4.1. Element Release Rates

Element release rates from biotite and calcium-rich feldspar were expected to be higher in treatments with ectomycorrhizal fungi than without fungi, and higher in all biological treatments than in the abiotic treatments [4,63]. It was also expected that the seedlings with ectomycorrhizal fungi would allocate more carbon below ground, accumulate larger biomass, and grow more successfully under base cation limitation than the seedlings without the fungi [19,64]. However, the latter could not be verified within these studies because some of the important controls did not survive in each experiment or the inoculation with EMF did not work well (Table 2). The results indicate that the red pine seedlings grew larger biomass in both ZS and BB experiments under the given laboratory conditions than the Scots pine seedlings, but the mycorrhizal colonization of Scots pine seedlings was more successful (Table 2). These large differences could indicate some species-specific responses to the growth conditions, but this needs to be tested in experiments where the two pine species are grown together in order to rule out other factors [65].

The net potassium release was similar for the KU and the BB experiments (Figure 2A). In the BB experiment, the abiotic, pine with bacteria only, and pine with mycorrhizal fungi treatments

released about the same amount of potassium, which can be explained by the watering regime that flushed the columns at every irrigation event [50] and provided a strong abiotic weathering signal; the relative element release ratio was nearly one (Figure 2C). By contrast, in the KU experiment, where the columns were flushed only at zero, three, six, and nine months, the relative potassium release was shown about three to five times higher rates of weathering in the columns with seedlings than the abiotic KU_A samples (Figure 2C). However, there were only slight differences among the three fungal treatments of the KU columns, which were all within the variability range of the replicates of each treatment (Figure 2A). In the ZS experiment, where fungal association with red pine was unsuccessful [49] and the water application was the lowest among the experiments, the net potassium release of the pine treatments remained similar to the abiotic ZS_A treatment (Figure 2A). In addition, the biotic enhancement ratio for potassium in the ZS experiment, where mycorrhization was minimal or none (Table 2), were nearly identical to the BB experiment (Figure 2C). These results support the interpretation that the weathering benefit of ectomycorrhizal association is magnified under low water availability [48], which was less in the KU than in the BB experiment. This has to be further tested in laboratory and field settings.

Biotite tends to dissolve and transform easily in any acidic environment [61,66–68], and increased dissolution rates have been demonstrated with the presence of organic acids, especially oxalate [61,69,70]. However, biotite persists in many soils, which indicates that biotite dissolution is incongruent in pH conditions common to soils and element release becomes diffusion-limited due to secondary phases/remnant silicate framework at the mineral surface [61]. Some agricultural studies showed that after tillage, the soils released more cations from clays [71], and in forests after disturbance, the cation nutrient release also increased for a short period of time [25,45,72], because these processes likely expose fresh mineral surfaces and enhance the temporary cation release from both primary and secondary minerals. However, with changing climate and water availability, the role of mycorrhizal associations in the nutrient acquisition of higher plants might increase in areas subjected to drier conditions in the future [73].

The net calcium release rate patterns are different among the experiments (Figure 2B). There was a much higher net release rate for calcium in the KU columns than in the other two experiments (Figure 2B), but the biotic enhancement rates for calcium were low and similar among the experiments ($p = 0.08$; Figure 2C). In the KU columns, the biotic enhancement rate was the greatest in the SP_PI treatment (Figure 3C). Schmalenberger et al. [74] reported that *P. involutus* is effective in mineral weathering because of the production of large amounts of oxalic acid, and this fungus is found in association with Scots pine in most natural environments [20]. Oxalic acid is known to have a high weathering effect on calcium-bearing minerals [70,74]. Although no calcium oxalate precipitates were observed on any imaged mineral surfaces (Figures 6 and 7), this does not exclude the possibility of the formation of these secondary minerals. In the red pine treatments, the variation of the calcium release ratios within treatments was larger than the differences among the treatments (Figure 2C). Calcium is thought to rarely be limiting in natural settings [18], but with the increased acidification of the environment as a result of the increase in carbon dioxide concentration in the atmosphere, as well as agricultural and silvicultural applications, many soils can be vulnerable to calcium and other base cation depletion [3,13]. Mycorrhizal fungi have the potential to bridge the gap between calcium availability and mineral sources, as suggested by the mineral calcium fertilization studies of the Hubbard Brook Experimental Forest in NH, USA [75].

Different fungal species did not cause striking differences in potassium and calcium release in the KU experiment, but they were substantially different from the abiotic treatment. By contrast, in the red pine experiments, the treatments with seedlings, ectomycorrhizal fungi, and with bacterial associates or without microbes were nearly identical to the abiotic treatments. These differences within the experiments imply a species-specific response of red pine vs. Scots pine to the base cation limiting conditions. Although, Scots pine seedlings in the KU experiment grew much less than red pine seedlings in the BB and ZS experiments (Table 2), Scots pine released more potassium from the biotite

(Figure 2). This could suggest a more active role of Scots pine compared to red pine in the weathering of silicates, but the two species need to be grown and compared in the same experiment to confirm this implication. The roots of Scots pine only explored about one third of the available soil volume in the columns, while red pine became root-bound in both the ZS and BB experiments after nine months. Scots pine seedlings without any fungal and/or bacterial inoculum (SP_UI treatment, $n = 10$) died between three and six months in the KU experiment. Does this indicate that Scots pine is only successful under base cation limitations if fungal and bacterial associates are present? Is mycorrhizal Scots pine more efficient in mineral dissolution than red pine under base cation limitations? There were no differences between the red pine treatments in the ZS and BB experiments (Figure 2), and they all grew relatively large biomass (Table 2). This suggests that the ectomycorrhizal fungi is of minor importance for red pine growth and perhaps red pine is well suited to cope with base cation limitations regardless of associated microbes. Balogh-Brunstad et al. [30] reported that ectomycorrhizal association increased red pine element release by approximately a factor of 2 relative to pine associations with bacteria only, but this observation was for the second six months of a 12-month experiment. This highlights the potential importance of time frame in comparisons of studies such as these.

4.2. Rhizospheric Mineral Alterations and Biofilm Formation

After nine months' incubation in the rhizosphere of Scots pine in the KU experiment, AFM showed shallow, 7- to 20-nm-deep, etched fungal hypha channels on biotite surfaces (Figures 3 and 4). There were etched channels on the biotite surfaces from all of the Scots pine treatments in the KU experiment. On the KU_A treatment (control), there was no evidence of biologically generated etched channels (Figure 3D). These results support the findings of others, that fungal hyphal growth alters the biotite surface both chemically and physically when direct attachment occurs [30,32–35]. Amplitude retrace (deflection) images help to visualize the shape of the surface-covering materials (Figure 5). These images show that biofilm/EPS formation was clearly observed in the SP_PI treatment (Figure 5A). Gazzè et al. [76] showed that *P. involutus* is able to produce EPS exudates even without bacterial associates, which is supported by our study (Figures 5A and 6E). Fungal hyphal attachment (Figure 5B) and extensive biofilm/EPS production (Figure 6D) were documented for *P. fallax* with SEM. However, observations of *S. bovinus* did not support our hypothesis of enhanced biofilm formation and/or fungal hyphal attachment to surfaces (Figures 5C and 6C). All these fungal species are described as able to weather silicates in soil environments in association with a host [20,24,41,51–54], which is supported by the bulk composition data, but surface attachment of fungal hyphae and biofilm/EPS coverage proved to be minor contributors to the potassium and calcium release under our experimental conditions.

The SEM images allowed a comparison of all three experiments and a large mineral surface area was investigated, which showed patchy biofilm/EPS development on both biotite and feldspar surfaces. Fungal hyphae and bacteria attachment to mineral surfaces were observed in all treatments with microbes (Figure 6A–F) and root hairs also adhered to biotite (Figure 6F). These observations support previous studies of rhizospheric minerals [22]. However, our hypotheses were not supported by the KU and ZS experiments because rhizospheric biofilm development was not dominant, and the biofilm did not incorporate much bacteria and fungi in the KU and ZS experiments. By contrast, the BB experiment exhibited more developed biofilm and EPS coverage in the rhizosphere (e.g., Figure 6A,B) and nearly 50% of all mineral surfaces investigated were covered by biofilm [30]. The KU experiment was only inoculated with the various fungi and some bacterial infection occurred because the seedlings were not grown in a sterile growth chamber. They remained relatively bacteria-free, which did not allow development of collaboration between plant roots, mycorrhizal fungi, and associated bacteria (Figure 1). In addition, the microscopic investigation only provided information at one snapshot in time when the columns were destructively sampled. Thus, the turnover rate of biological material in the rhizosphere was not assessed. All experiments showed carbon deposition to the rhizosphere, which agrees with the results presented by Dohnalkova et al. [77].

The proportion of the observed channel-shaped etching pattern area with SEM (Figure 7A,B) was semi-quantitatively estimated, and the results indicated species-specific differences among the fungal treatments, RP_ST_E (21%), RP_PT_BP (11%), SP_PF (9%), SP_PI (4%), and SP_SB (1%), which agrees with the biological cover observations but not with the bulk composition data. Thus, in these experiments, the direct surface attachment and etching by fungal hyphae are not the most significant contributors to the potassium and calcium release from the minerals. These findings support field studies that propose that mycorrhizal weathering is important where the direct contribution of surface-attached fungi to biological and total weathering rates remains low [42,43]. Overall, the bulk chemical analysis and microscopy investigations of the mineral grains revealed that while the fungal species promoted dissolution of the mineral surfaces, no species-specific differences were observed among the mycorrhizal fungi.

Dissolution of minerals was greater in the biological treatments than in the abiotic treatments in the KU and ZS experiments, which is consistent with the observation of accumulated secondary precipitates (Figure 7C–F). This is also consistent with the dramatic decrease in pH of drainage in the biological treatments of those experiments. Why the drainage pH did not also drop in the BB experiment is not clear, but might be related to the greater production of biofilm, under which weathering and pH buffering were hypothesized to occur, in the BB treatments with pine. However, the neutrality of the BB drainage pH could also result from other factors, including shorter drainage residence time in the columns by the application of large amounts of water.

5. Conclusions

The hypothesis about the importance of fungal attachment under the cover of biofilm was not clearly supported by this comparison study. Although we found clear evidence that ectomycorrhizal fungi stimulate silicate weathering in the KU and BB experiments, this effect was minor compared to other environmental conditions, such as water application (rain events), which varied among the experiments. The minor effect of biofilm formation on the overall weathering budgets suggests that such detailed information might not be necessary to describe weathering rates in long-term (geologic) weathering models [37]. However, on time scales of ecosystem development, such details might be important, as noted by Balogh-Brunstad et al. [30] who found that the ectomycorrhizal association was associated with a strong reduction of the element drainage (loss) flux relative to the total element release flux during months 6–12 of the BB experiment. Thus, the potential importance of timeframe for the development of the relationships suggested in Figure 1 must also be acknowledged. In addition, the results indicate that the pine species might differ in their influence on silicate mineral weathering under potassium and calcium limitations, and that mycorrhizal fungi respond to different water availabilities in the growth medium. The latter is consistent with the idea that the primary positive effect of mycorrhizal fungi on nutrient uptake has to do with the regulation of water transport and availability under low water content [48]. However, to fully evaluate the effect of ectomycorrhizal fungi in relation to watering regimes and other environmental factors, as well as species-specificity of trees and fungi in weathering, new experiments need to be designed and performed where these factors are investigated under controlled conditions. Such experiments are strongly encouraged.

Supplementary Materials: The following are available online at http://www.mdpi.com/2411-5126/1/1/5/s1; Table S1: Recipe for Marx Melin-Norkrans Agar; Table S2: Nutrient solution composition of the KU experiment; Table S3: Estimated geometric surface area of biotite and calcium-feldspar in each experiment; Table S4: Data in mmol used for the mass balance calculations of the element release calculations; Table S5: Summary of ANOVA results.

Acknowledgments: This research was supported by: the People Programme (Marie Curie Actions) of the European Union's Seventh Framework Programme FP7/2007-2013/ under REA grant agreement nº 235879 to Balogh-Brunstad; by the NSF/EAR 03-12011 and 09-52399 to Keller; and NSF/EAR 09-52052 to Balogh-Brunstad. A portion of this research was performed at the Environmental Molecular Science Laboratory, at Pacific Northwest National Laboratory, Richland, WA with the help of Alice Dohnalkova and Bruce Arey. Some SEM work was completed at the Department of Geology, Colgate University, NY with the help of Di Keller. The authors thank the NanoGeoScience laboratory at the University of Copenhagen (KU), Denmark, and the Microbial Ecology

facilities at Lund University (LU), Sweden for providing space, materials, and equipment to perform the KU column experiments. Special thanks goes to Tue Hassenkam for AFM, Kim Dalby for SEM and Sorin Nedel for helping with the chemical analysis at KU and Nicholas Rosenstock for helping with the inoculation process at LU. The authors also thank the WSU Geoanalytical Lab for the chemical analysis of the minerals and other members of the WSU research team: Daryl Stacks (undergraduate student), Michael Grant (PhD student), Linda Thomashow and James Harsh (PIs on NSF grant) for working with the WSU column experiment. Kyle Greenberg and Sheila Niedziela, undergraduates at Hartwick College, completed a portion of the microscopy work. We thank Andrew Bray and two anonymous reviewers who provided constructive comments that helped to improve the manuscript.

Author Contributions: Z.B.-B., C.K.K. and H.W. conceived and designed the experiments; Z.B.-B. and Z.S. performed the experiments; Z.B.-B., C.K.K., Z.S., H.W. and S.L.S.S. worked together to analyze the data; S.L.S.S. contributed materials, space and analytical equipment; H.W. also provided materials and space; Z.B.-B. and C.K.K. wrote the paper with input from all authors. All authors read and approved the content.

Conflicts of Interest: The authors declare no conflict of interest.

References

1. Beerling, D.J.; Berner, R.A. Feedbacks and the coevolution of plants and atmospheric CO_2. *Proc. Natl. Acad. Sci. USA* **2005**, *102*, 1302–1305. [CrossRef] [PubMed]
2. Brantley, S.L.; Goldhaber, M.B.; Ragnarsdottir, K.V. Crossing disciplines and scales to understand the critical zone. *Elements* **2007**, *3*, 307–314. [CrossRef]
3. Banwart, S.A.; Berg, A.; Beerling, D.J. Process-based modeling of silicate mineral weathering responses to increasing atmospheric CO_2 and climate change. *Glob. Biogeochem. Cycles* **2009**, *23*. [CrossRef]
4. Landeweert, R.; Hoffland, E.; Finlay, R.D.; Kuyper, T.W.; van Breemen, N. Linking plants to rocks: Ectomycorrhizal fungi mobilize nutrients from minerals. *Trends Ecol. Evol.* **2001**, *16*, 248–254. [CrossRef]
5. Bornyasz, M.A.; Graham, R.C.; Allen, M.F. Ectomycorrhizae in a soil-weathered granitic bedrock regolith: Linking matrix resources to plants. *Geoderma* **2005**, *126*, 141–160. [CrossRef]
6. Van Hees, P.A.W.; Rosling, A.; Lundström, U.S.; Finlay, R.D. The biogeochemical impact of ectomycorrhizal conifers on major soil elements (Al, Fe, K and Si). *Geoderma* **2006**, *136*, 364–377. [CrossRef]
7. Finlay, R.; Wallander, H.; Smits, M.; Holmstrom, S.; Van Hess, P.; Lian, B.; Rosling, A. The role of fungi in biogenic weathering in boreal forest soils. *Fungal Biol. Rev.* **2009**, *23*, 101–106. [CrossRef]
8. Turpault, M.-P.; Nys, C.; Calvaruso, C. Rhizosphere impact on the dissolution of test minerals in a forest ecosystem. *Geoderma* **2009**, *153*, 147–154. [CrossRef]
9. Koele, N.; Turpault, M.P.; Hildebrand, E.E.; Uroz, S.; Frey-Klett, P. Interactions between mycorrhizal fungi and mycorrhizosphere bacteria during mineral weathering: Budget analysis and bacterial quantification. *Soil Biol. Biochem.* **2009**, *41*, 1935–1942. [CrossRef]
10. Koele, N.; Dickie, I.A.; Blum, J.D.; Gleason, J.D.; de Graaf, L. Ecological significance of mineral weathering in ectomycorrhizal and arbuscular mycorrhizal ecosystems from a field-based comparison. *Soil Biol. Biochem.* **2014**, *69*, 63–70. [CrossRef]
11. Calvaruso, C.; Collignon, C.; Kies, A.; Turpault, M.P. Seasonal evolution of the rhizosphere effect on major and trace elements in soil solutions of Norway Spruce (*Picea abies Karst*) and beech (*Fagus sylvatica*) in an acidic forest soil. *Open J. Soil Sci.* **2014**, *4*, 323–336. [CrossRef]
12. Meheruna, A.; Akagi, T. Role of fine roots in the plant-induced weathering of andesite for several plant species. *Geochem. J.* **2006**, *40*, 57–67. [CrossRef]
13. Hinsinger, P.; Bengough, A.G.; Vetterlein, D.; Young, I.M. Rhizosphere: Biophysics, biogeochemistry and ecological relevance. *Plant Soil* **2009**, *321*, 117–152. [CrossRef]
14. Hinsinger, P. Plant-induced changes in soil processes and properties. In *Soil Conditions and Plant Growth*; Gregory, P.J., Nortcliff, S., Eds.; Blackwell Publishing Ltd.: Oxford, UK, 2013; pp. 323–365. ISBN 978-1-4051-9770-0. [CrossRef]
15. Brantley, S.L.; Megonigal, J.P.; Scatena, F.N.; Balogh-Brunstad, Z.; Barnes, R.T.; Bruns, M.A.; Van Cappellen, P.; Dontsova, K.; Hartnett, H.E.; Hartshorn, A.S.; et al. Twelve testable hypotheses on the geobiology of weathering. *Geobiology* **2011**, *9*, 140–165. [CrossRef] [PubMed]
16. McNear, D.H., Jr. The rhizosphere-roots, soil and everything in between. *Nat. Educ. Knowl.* **2013**, *4*, 1.
17. National Research Council (NRC). *Basic Research Opportunities in Earth Sciences*; The National Academies Press: Washington, DC, USA, 2001; p. 154.

18. Marschner, H. *Marschner's Mineral Nutrition of Higher Plants*; Academic Press: London, UK, 2011; ISBN 978-0-12-384905-2.
19. Smith, S.E.; Read, D.J. *Mycorrhizal Symbiosis*, 3rd ed.; Academic Press: London, UK, 2010; ISBN 978-0-12-370526-6.
20. Van Schöll, L.; Kuyper, T.W.; Smits, M.M.; Landeweert, R.; Hoffland, E.; Van Breemen, N. Rock-eating mycorrhizas: Their role in plant nutrition and biogeochemical cycles. *Plant Soil* **2008**, *303*, 35–47. [CrossRef]
21. Leake, J.R.; Duran, A.L.; Hardy, K.E.; Johnson, I.; Beerling, D.J.; Banwart, S.A.; Smits, M.M. Biological weathering in soil: The role of symbiotic root-associated fungi biosensing minerals and directing photosynthate-energy into grain-scale mineral weathering. *Mineral. Mag.* **2008**, *72*, 85–89. [CrossRef]
22. Cheng, L.; Chen, W.; Adams, T.S.; Wei, X.; Li, L.; McCormack, M.L.; DeForest, J.L.; Koide, R.T.; Eissenstat, D.M. Mycorrhizal fungi and roots are complementary in foraging within nutrient patches. *Ecology* **2016**, *97*, 2815–2823. [CrossRef] [PubMed]
23. Jongmans, A.G.; Van Breemen, N.; Lundström, U.; Van Hees, P.A.W.; Finlay, R.D.; Srinivasan, M.; Unestam, T.; Giesler, R.; Melkerud, P.A.; Olsson, M. Rock-eating fungi. *Nature* **1997**, *389*, 682–683. [CrossRef]
24. Van Breemen, N.; Finlay, R.; Lundström, U.; Jongmans, A.G.; Giesler, R.; Olsson, M. Mycorrhizal weathering: A true case of mineral plant nutrition? *Biogeochemistry* **2000**, *49*, 53–67. [CrossRef]
25. Blum, J.D.; Klaue, A.; Nezat, C.A.; Driscoll, C.T.; Johnson, C.E.; Siccama, T.G.; Eagar, C.; Fahey, T.J.; Likens, G.E. Mycorrhizal weathering of apatite as an important calcium source in base-poor forest ecosystems. *Nature* **2002**, *417*, 729–731. [CrossRef] [PubMed]
26. Hoffland, E.; Giesler, R.; Jongmans, T.; Van Breemen, N. Increasing feldspar tunneling by fungi across a north Sweden podzol chronosequence. *Ecosystems* **2002**, *5*, 11–22. [CrossRef]
27. Smits, M.M.; Hoffland, E.; Jongmans, A.G.; van Breemen, N. Contribution of mineral tunneling to total feldspar weathering. *Geoderma* **2005**, *125*, 59–69. [CrossRef]
28. Calvaruso, C.; Turpault, M.P.; Leclerc, E.; Frey-Klett, P. Impact of ectomycorrhizosphere on the functional diversity of soil bacterial and fungal communities from a forest stand in relation to nutrient mobilization processes. *Microb. Ecol.* **2007**, *54*, 567–577. [CrossRef] [PubMed]
29. Frey-Klett, P.; Garbaye, J.A.; Tarkka, M. The mycorrhiza helper bacteria revisited. *New Phytol.* **2007**, *176*, 22–36. [CrossRef] [PubMed]
30. Balogh-Brunstad, Z.; Keller, C.K.; Gill, R.A.; Bormann, B.T.; Li, C.Y. The effect of bacteria and fungi on chemical weathering and chemical denudation fluxes in pine growth experiments. *Biogeochemistry* **2008**, *88*, 153–167. [CrossRef]
31. Courty, P.E.; Buée, M.; Diedhiou, A.G.; Frey-Klett, P.; Le Tacon, F.; Rineau, F.; Turpault, M.P.; Uroz, S.; Garbaye, J. The role of ectomycorrhizal communities in forest ecosystem processes: New perspectives and emerging concepts. *Soil Biol. Biochem.* **2010**, *42*, 679–698. [CrossRef]
32. Bonneville, S.; Smits, M.M.; Brown, A.; Harrington, J.; Leake, J.R.; Brydson, R.; Benning, L.G. Plant-driven fungal weathering: Early stages of mineral alteration at the nanometer scale. *Geology* **2009**, *37*, 615–618. [CrossRef]
33. Bonneville, S.; Morgan, D.J.; Schmalenberger, A.; Bray, A.; Brown, A.; Banwart, S.A.; Benning, L.G. Tree-mycorrhiza symbiosis accelerate mineral weathering: Evidences from nanometerscale elemental fluxes at the hypha–mineral interface. *Geochim. Cosmochim. Acta* **2011**, *75*, 6988–7005. [CrossRef]
34. McMaster, T.J. Atomic Force Microscopy of the fungi–mineral interface: Applications in mineral dissolution, weathering and biogeochemistry. *Curr. Opin. Biotechnol.* **2012**, *23*, 562–569. [CrossRef] [PubMed]
35. Saccone, L.; Gazzè, S.A.; Duran, A.L.; Leake, J.R.; Banwart, S.A.; Ragnarsdóttir, K.V.; Smits, M.M.; McMaster, T.J. High resolution characterization of ectomycorrhizal fungal-mineral interactions in axenic microcosm experiments. *Biogeochemistry* **2012**, *111*, 411–425. [CrossRef]
36. Gazzè, S.A.; Saccone, L.; Vala Ragnarsdottir, K.; Smits, M.M.; Duran, A.L.; Leake, J.R.; Banwart, S.A.; McMaster, T.J. Nanoscale channels on ectomycorrhizal-colonized chlorite: Evidence for plant-driven fungal dissolution. *J. Geophys. Res. Biogeosci.* **2012**, *117*, G00N09. [CrossRef]
37. Sverdrup, H. Chemical weathering of soil minerals and the role of biological processes. *Fungal Biol. Rev.* **2009**, *23*, 94–100. [CrossRef]
38. Ward, M.B.; Kapitulčinová, D.; Brown, A.P.; Heard, P.J.; Cherns, D.; Cockell, C.S.; Hallam, K.R.; Ragnarsdóttir, K.V. Investigating the role of microbes in mineral weathering: Nanometre-scale characterisation of the cell–mineral interface using FIB and TEM. *Micron* **2013**, *47*, 10–17. [CrossRef] [PubMed]

39. Smits, M.M.; Johansson, L.; Wallander, H. Soil fungi appear to have a retarding rather than a stimulating role on soil apatite weathering. *Plant Soil* **2014**, *385*, 217–228. [CrossRef]
40. Li, Z.; Liu, L.; Chen, J.; Teng, H.H. Cellular dissolution at hypha-and spore-mineral interfaces revealing unrecognized mechanisms and scales of fungal weathering. *Geology* **2016**, *44*, 319–322. [CrossRef]
41. Rosenstock, N.P.; Berner, C.; Smits, M.M.; Krám, P.; Wallander, H. The role of phosphorus, magnesium and potassium availability in soil fungal exploration of mineral nutrient sources in Norway spruce forests. *New Phytol.* **2016**, *211*, 542–553. [CrossRef] [PubMed]
42. Smits, M.M.; Bonneville, S.; Haward, S.; Leake, J.R. Ectomycorrhizal weathering, a matter of scale? *Mineral. Mag.* **2008**, *72*, 131–134. [CrossRef]
43. Smits, M.M.; Herrmann, A.M.; Duane, M.; Duckworth, O.W.; Bonneville, S.; Benning, L.G.; Lundström, U. The fungal–mineral interface: Challenges and considerations of micro-analytical developments. *Fungal Biol. Rev.* **2009**, *23*, 122–131. [CrossRef]
44. Augustin, F.; Houle, D.; Gagnon, C.; Courchesne, F. Long-term base cation weathering rates in forested catchments of the Canadian Shield. *Geoderma* **2015**, *247*, 12–23. [CrossRef]
45. Balogh-Brunstad, Z.; Keller, C.K.; Bormann, B.T.; O'Brien, R.; Wang, D.; Hawley, G. Chemical weathering and chemical denudation dynamics through ecosystem development and disturbance. *Glob. Biogeochem. Cycles* **2008**, *22*, GB1007. [CrossRef]
46. Taylor, L.L.; Leake, J.R.; Quirk, J.; Hardy, K.; Banwart, S.A.; Beerling, D.J. Biological weathering and the long-term carbon cycle: Integrating mycorrhizal evolution and function into the current paradigm. *Geobiology* **2009**, *7*, 171–191. [CrossRef] [PubMed]
47. Hasenmueller, E.A.; Gu, X.; Weitzman, J.N.; Adams, T.S.; Stinchcomb, G.E.; Eissenstat, D.M.; Drohan, P.J.; Brantley, S.L.; Kaye, J.P. Weathering of rock to regolith: The activity of deep roots in bedrock fractures. *Geoderma* **2017**, *300*, 11–31. [CrossRef]
48. Li, T.; Lin, G.; Zhang, X.; Chen, Y.; Zhang, S.; Chen, B. Relative importance of an arbuscular mycorrhizal fungus (*Rhizophagus intraradices*) and root hairs in plant drought tolerance. *Mycorrhiza* **2014**, *24*, 595–602. [CrossRef] [PubMed]
49. Shi, Z.; Balogh-Brunstad, Z.; Grant, M.; Harsh, J.; Gill, R.; Thomashow, L.; Dohnalkova, A.; Stacks, D.; Letourneau, M.; Keller, C.K. Cation uptake and allocation by red pine seedlings under cation-nutrient stress in a column growth experiment. *Plant Soil* **2014**, *378*, 83–98. [CrossRef]
50. Balogh, Z. Chemical Hydrology of Vascular Plant Growth: Role of Root-Fungus Associations. Doctoral Dissertation, Washington State University, Pullman, WA, USA, 2006.
51. Wallander, H.; Wickman, T. Biotite and microcline as potassium sources in ectomycorrhizal and non-mycorrhizal *Pinus sylvestris* seedlings. *Mycorrhiza* **1999**, *9*, 25–32. [CrossRef]
52. Glowa, K.R.; Arocena, J.M.; Massicotte, H.B. Extraction of potassium and/or magnesium from selected soil minerals by Piloderma. *Geomicrobiol. J.* **2003**, *20*, 99–111. [CrossRef]
53. Van Schöll, L.; Hoffland, E.; Van Breemen, N. Organic anion exudation by ectomycorrhizal fungi and *Pinus sylvestris* in response to nutrient deficiencies. *New Phytol.* **2006**, *170*, 153–163. [CrossRef] [PubMed]
54. Van Schöll, L.; Smits, M.M.; Hoffland, E. Ectomycorrhizal weathering of the soil minerals muscovite and hornblende. *New Phytol.* **2006**, *171*, 805–814. [CrossRef] [PubMed]
55. Marx, D.H. The influence of ectotrophic mycorrhizal fungi on the resistance of pine roots to pathogenetic infection. I. Antagonism of mycorrhizal fungi to root pathogenic fungi and soil bacteria. *Phytopathology* **1969**, *59*, 159–163.
56. Johnson, D.M.; Hooper, P.R.; Conrey, R.M. XRF analysis of rocks and minerals for major and trace elements on a single low dilution Li-tetraborate fused bead. *Adv. X-Ray Anal.* **1999**, *41*, 843–867.
57. Deer, W.A.; Howie, R.A.; Zussman, J. *An Introduction to the Rock-Forming Minerals*, 2nd ed.; Longman: London, UK, 1992.
58. Peterson, R.L.; Massicotte, H.B.; Melville, L.H. *Mycorrhizas: Anatomy and Cell Biology*; NRC Research Press: Ottawa, ON, Canada, 2004.
59. SW-846 EPA Method 3050B, Acid digestion of sediments, sludges, and soils. In *Test Methods for Evaluating Solid Waste*, 3rd ed.; U.S. EPA: Washington, DC, USA, 1995.
60. McIntosh, J.L. Bray and Morgan soil test extractants modified for testing acid soils from different parent materials. *Agron. J.* **1969**, *61*, 259–265. [CrossRef]

61. Bray, A.W.; Oelkers, E.H.; Bonneville, S.; Wolff-Boenisch, D.; Potts, N.J.; Fones, G.; Benning, L.G. The effect of pH, grain size, and organic ligands on biotite weathering rates. *Geochim. Cosmochim. Acta* **2015**, *164*, 127–145. [CrossRef]
62. Hodson, M.E. Searching for the perfect surface area normalizing term—A comparison of BET surface area, geometric surface area-and mass-normalized dissolution rates of anorthite and biotite. *J. Geochem. Explor.* **2006**, *88*, 288–291. [CrossRef]
63. Lamb, R.J.; Richards, B.N. Effect of mycorrhizal fungi on the growth and nutrient status of slash and radiata pine seedlings. *Aust. For.* **1971**, *35*, 1–7. [CrossRef]
64. Leake, J.; Johnson, D.; Donnelly, D.; Muckle, G.; Boddy, L.; Read, D. Networks of power and influence: The role of mycorrhizal mycelium in controlling plant communities and agroecosystem functioning. *Can. J. Bot.* **2004**, *82*, 1016–1045. [CrossRef]
65. Wallander, H.; Nylund, J.E. Effects of excess nitrogen on carbohydrate concentration and mycorrhizal development of *Pinus sylvestris* L. seedlings. *New Phytol.* **1991**, *119*, 405–411. [CrossRef]
66. Wallander, H.; Hagerberg, D. Do ectomycorrhizal fungi have a significant role in weathering of minerals in forest soil? *Symbiosis* **2004**, *37*, 249–257.
67. Calvaruso, C.; Mareschal, L.; Turpault, M.P.; Leclerc, E. Rapid clay weathering in the rhizosphere of Norway spruce and oak in an acid forest ecosystem. *Soil Sci. Soc. Am. J.* **2009**, *73*, 331–338. [CrossRef]
68. Pinzari, F.; Cuadros, J.; Napoli, R.; Canfora, L.; Bardají, D.B. Routes of phlogopite weathering by three fungal strains. *Fungal Biol.* **2016**, *120*, 1582–1599. [CrossRef] [PubMed]
69. Li, J.; Zhang, W.; Li, S.; Li, X.; Lu, J. Effects of citrate on the dissolution and transformation of biotite, analyzed by chemical and atomic force microscopy. *Appl. Geochem.* **2014**, *51*, 101–108. [CrossRef]
70. Haward, S.J.; Smits, M.M.; Ragnarsdóttir, K.V.; Leake, J.R.; Banwart, S.A.; McMaster, T.J. In situ atomic force microscopy measurements of biotite basal plane reactivity in the presence of oxalic acid. *Geochim. Cosmochim. Acta* **2011**, *75*, 6870–6881. [CrossRef]
71. Munkholm, L.J.; Heck, R.J.; Deen, B. Long-term rotation and tillage effects on soil structure and crop yield. *Soil Tillage Res.* **2013**, *127*, 85–91. [CrossRef]
72. Keller, C.K.; O'brien, R.; Havig, J.R.; Smith, J.L.; Bormann, B.T.; Wang, D. Tree harvest in an experimental sand ecosystem: Plant effects on nutrient dynamics and solute generation. *Ecosystems* **2006**, *9*, 634–646. [CrossRef]
73. Phillips, R.P.; Ibanez, I.; D'Orangeville, L.; Hanson, P.J.; Ryan, M.G.; McDowell, N.G. A belowground perspective on the drought sensitivity of forests: Towards improved understanding and simulation. *For. Ecol. Manag.* **2016**, *380*, 309–320. [CrossRef]
74. Schmalenberger, A.; Duran, A.L.; Bray, A.W.; Bridge, J.; Bonneville, S.; Benning, L.G.; Romero-Gonzalez, M.E.; Leake, J.R.; Banwart, S.A. Oxalate secretion by ectomycorrhizal *Paxillus involutus* is mineral-specific and controls calcium weathering from minerals. *Sci. Rep.* **2015**, *5*, 12187. [CrossRef] [PubMed]
75. Phillips, R.P.; Fahey, T.J. Fertilization effects on fineroot biomass, rhizosphere microbes and respiratory fluxes in hardwood forest soils. *New Phytol.* **2007**, *176*, 655–664. [CrossRef] [PubMed]
76. Gazzè, S.A.; Saccone, L.; Smits, M.M.; Duran, A.L.; Leake, J.R.; Banwart, S.A.; Ragnarsdottir, K.V.; McMaster, T.J. Nanoscale observations of extracellular polymeric substances deposition on phyllosilicates by an ectomycorrhizal fungus. *Geomicrobiol. J.* **2013**, *30*, 721–730. [CrossRef]
77. Dohnalkova, A.C.; Tfaily, M.M.; Smith, A.P.; Chu, R.; Crump, A.; Brislawn, C.J.; Varga, T.; Shi, Z.; Thomashow, L.S.; Harsh, J.B.; et al. Molecular and Microscopic Insights into the Persistence of Soil Organic Matter in a Red Pine Rhizosphere. *Soils* **2017**, *1*, 4. [CrossRef]